Human Movement Science 86 (2022) 103020

Contents lists available at ScienceDirect

Human Movement Science

journal homepage: www.elsevier.com/locate/humov

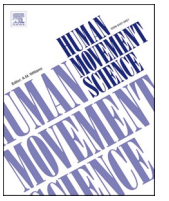

Transformation from arm joint coordinates to hand external coordinates explains non-uniform precision of hand position sense in horizontal workspace

Kyunggeune Oh [a,b,c], Boris I. Prilutsky [a,*]

[a] School of Biological Sciences, Georgia Institute of Technology, Atlanta, GA 30332-0356, USA
[b] Center for Movement Studies, Kennedy Krieger Institute, Baltimore, MD 21205, USA
[c] Department of Neuroscience, Johns Hopkins University, Baltimore, MD 21205, USA

ARTICLE INFO

Keywords:
Hand position sense
Joint to hand coordinate transformation
Precision ellipse
Arm stiffness

ABSTRACT

People perceive hand position in horizontal workspace more precisely in radial than in azimuth directions and closer to the body than farther away. Current explanations for this position sense non-uniformity include spatial asymmetry in arm proprioceptive activities and/or cortex maps, experience-dependent learning, arm posture, and others. Here we investigated contributions to this non-uniformity of a posture-dependent transformation from arm joint angles, sensed by arm proprioceptors, to hand position. We measured precision of hand position sense in a bimanual hand mirror-position matching task at four horizontal targets forming a square in front of the body in 11 blindfolded individuals. We found lower hand precision in azimuth than in radial direction, higher azimuth precision at close targets, and higher radial precision at distant targets. We then theoretically analyzed the transformation of random angle errors at shoulder and elbow into hand position random errors in a horizontal plane and obtained similar distributions of hand position errors. The predicted and experimental hand-precision ellipse orientations, but not ellipse shapes or sizes, were highly correlated and were nearly orthogonal to arm stiffness ellipse orientations reported in the literature. We concluded that the joint-to-hand coordinate transformation is responsible for the non-uniform precision of hand position sense.

1. Introduction

Position sense of the body limbs is critical for the accurate control of posture and movement and for the appropriate responses to sudden external perturbations. The lack of position sense due to illness has devastating consequences for the performance of even simplest motor tasks (Cole & Paillar, 1998; Sainburg, Poizner, & Ghez, 1993; Sarlegna, Gauthier, Bourdin, Vercher, & Blouin, 2006). Although many sensory systems (visual, vestibular, tactile, and proprioceptive) and voluntary motor commands contribute to limb position sense, the muscle spindle and cutaneous afferents appear to be the major contributors to perception of joint angles and position of limb segments with respect to each other (Aimonetti, Hospod, Roll, & Ribot-Ciscar, 2007; Collins, Refshauge, Todd, & Gandevia, 2005; Feldman, 2011; Matthews, 1988; Plooy, Tresilian, Mon-Williams, & Wann, 1998; Proske, 2015; Proske & Gandevia, 2012).

* Corresponding author.
E-mail address: boris.prilutsky@ap.gatech.edu (B.I. Prilutsky).

https://doi.org/10.1016/j.humov.2022.103020
Received 5 May 2022; Received in revised form 17 October 2022; Accepted 23 October 2022
0167-9457/© 2022 Elsevier B.V. All rights reserved.

Hand position sense, which requires a transformation from perceived joint angular positions to hand Cartesian position, has been the focus of extensive studies. It has been shown experimentally that precision (random errors) of hand position sense is not uniform in a horizontal workspace. Specifically, the hand position is perceived more precisely in the radial than in the azimuth direction and closer to the body than farther away (Kuling, van der Graaff, Brenner, & Smeets, 2017; Rincon-Gonzalez, Buneo, & Helms Tillery, 2011; Rossetti, Meckler, & Prablanc, 1994; Slinger & Horsley, 1906; van Beers, Sittig, & Denier van der Gon, 1998; Wilson, Wong, & Gribble, 2010). Several explanations for the observed non-uniform precision of hand position sense have been suggested. Based on a qualitative graphical analysis of uncertainty of angular position at the shoulder and elbow joints in two arm postures (Fig. 1), a seminal study by van Beers and colleagues (van Beers et al., 1998) suggested that arm posture might be partially responsible for the non-uniform precision of hand position sense. Although that analysis seemed to provide some intuition for the experimentally obtained shape, orientation and size of the error distribution ellipse of the hand position at an extended and flexed arm posture (Fig. 1, black ellipses), it lacked rigor and employed questionable geometric manipulations. To show how the joint angular position uncertainties contribute to the hand error distribution, the authors fitted the experimentally obtained hand error distribution (hand precision ellipse) within the ranges of the shoulder and elbow joint uncertainties. To do that they placed the shoulder uncertainty range around the vertical line instead of placing it around the distal segment (the upper arm), as was done for the uncertainty range of the elbow (Fig. 1). As a result, the authors concluded that variation in the shoulder and elbow angles could explain the distribution of random hand position errors found experimentally and that the hand error distribution depended on arm posture (black ellipses in Fig. 1). As can be seen in Fig. 1B, this conclusion is inaccurate. Using the same graphical method and the proper placement of the shoulder angle uncertainties along the upper arm, one obtains a hand precision ellipse with a much larger area and different orientation and shape (compare the black and gray ellipse). In addition, one should expect that a single hand precision ellipse should fit into the shoulder and elbow uncertainty ranges in a plane. Fig. 1A (color ellipses) demonstrates that it is possible to fit multiple ellipses into the same joint uncertainty ranges by manipulating orientation, shape and size of the ellipses in a graphics software.

Scott and Loeb (Scott & Loeb, 1994) have also demonstrated effects of arm posture on the hand error distribution along a single line connecting the shoulder joint and hand using a musculoskeletal model of the arm and different assumptions about muscle spindle sensitivity and spindle distributions in one- and two-joint muscles. Besides analyzing hand errors along a single line, the authors obtained theoretical estimates of joint random errors and the corresponding hand position errors that were an order of magnitude smaller than found experimentally.

As no convincing explanations for the non-uniform precision of hand position sense were available, subsequent studies attempted to address this issue. Two of later studies (I. S. Howard, Ingram, Kording, & Wolpert, 2009; Rincon-Gonzalez et al., 2011) have proposed that the non-uniform precision of hand position sense in the arm workspace (i.e., higher precision near the body than farther away) is experience-dependent and results from the more frequent daily use of hands in close proximity to the body. Other proposed

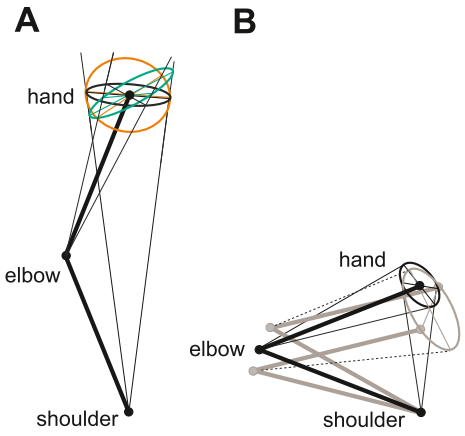

Fig. 1. Distribution of random errors of hand position sense (precision ellipses) in two arm postures derived by fitting ellipses into ranges of angular position uncertainties at the shoulder and elbow joints (modified with permission from Fig. 8 in (van Beers et al., 1998)). Black thick lines indicate arm segments; black thin straight lines indicate the angular uncertainty ranges at the shoulder and elbow joints as defined in (van Beers et al., 1998); black ellipses are uncertainties in the hand position (hand precision ellipses) fitted into joint angle uncertainties (van Beers et al., 1998). A: An extended arm posture with assumed shoulder and elbow joint uncertainties and multiple hand precision ellipses. The black ellipse is taken from (van Beers et al., 1998). The brown and green ellipses of different orientations and sizes are fitted in the same uncertainty ranges at the shoulder and elbow by manipulating the ellipse orientation, size and shape in the graphics software CorelDRAW 2018 (Corel Corporation, Canada). B: A flexed arm posture (thick black lines) with assumed shoulder and elbow joint uncertainties (thin continuous black lines) and a hand precision ellipse fitted into these joint uncertainties (black ellipse); reproduced with permission from (van Beers et al., 1998). Note that the shoulder joint uncertainty range is oriented vertically, whereas the elbow uncertainty range is oriented along the distal segment (forearm). Thick gray lines depict two arm flexed postures obtained by placing the upper arm at the edges of the shoulder uncertainty range oriented along the upper arm. The thin dashed lines depict a half of the elbow uncertainty range added to the two forearm orientations obtained by placing the upper arm along the edges of the shoulder uncertainty range. The gray ellipse is fitted into the thus obtained joint uncertainty ranges. See text for more explanations. (For interpretation of the references to color in this figure legend, the reader is referred to the web version of this article.)

explanations for the non-uniform precision of hand position sense include arm posture comfort (Rossetti et al., 1994), the spatial biases of muscle spindle and cutaneous afferent activity (Aimonetti, Roll, Hospod, & Ribot-Ciscar, 2012; Ribot-Ciscar, Bergenheim, Albert, & Roll, 2003; Wilson et al., 2010), the asymmetric spatial structure of the cortex proprioceptive map of the arm (Rincon-Gonzalez et al., 2011), and muscle spindle distribution in and interactions among one- and two-joint muscles (Scott & Loeb, 1994; Sturnieks, Wright, & Fitzpatrick, 2007).

Since hand position perception without vision requires a nonlinear transformation from joint coordinates to hand Cartesian coordinates, we hypothesized that the non-uniform precision of hand position sense in a horizontal workspace results from a nonlinear transformation of random errors in arm joint angles to errors in hand position. To test this hypothesis, we measured distributions of random errors of hand position sense in a horizontal plane in a group of blindfolded subjects and compared the experimental error distributions with errors distributions derived theoretically from the transformation of joint errors to hand position errors in a geometric arm model.

2. Methods

2.1. Hand mirror-position matching experiment

We conducted a hand mirror-position matching experiment to determine the precision of hand mirror-position sense at four locations in a horizontal space in front of the body (Fig. 2A) and compared the experimentally found precision with the precision of the hand position predicted by the arm geometric model.

2.1.1. Subjects

All subjects in this study were right-handed, as determined based on the Edinburgh Handedness Inventory (Oldfield, 1971), over the age of 18 years, and had no known history of neurological or musculoskeletal disorders. We recruited 11 individuals (seven males and four females; age 27.2 ± 11.4 years; Table 1). The experimental procedures of this study were consistent with the Ethical Principles for Medical Research Involving Human Subjects described in the Declaration of Helsinki and were approved by the Institutional Review Board of the Georgia Institute of Technology (protocol number H11212). All subjects read and signed written informed consent to participate in the study.

2.1.2. Experimental task

The subjects performed a bilateral hand mirror-position matching task while they were seated in the chair of the Kinarm exoskeleton robot (BKIN Technologies Ltd., Kingston ON, Canada) with both arms supported by the exoskeleton arms in a horizontal workspace. Before the task, the subject's arms were secured in a pronated position in the Kinarm robotic arms, and the vertical axis of the rotation of the shoulder and elbow joints of each arm was aligned with the corresponding joints of the Kinarm. The wrist joints were fixed. The Kinarm was calibrated according to established procedures.

At the beginning of each trial, the Kinarm moved both hands of the subject to the initial positions in front of the corresponding shoulder to make the elbow angle 90^o (Fig. 2A). After a short delay (1 s), the Kinarm moved the right hand of the subject to one of the four target positions over a period of 1 s in random order. The target locations for the right arm were: (1) 45^o from the left-right axis in a counterclockwise direction, T1; (2) 135^o, T2; (3) 225^o, T3; and (4) 315^o, T4. The subject had to match the distance and mirror direction of the right index finger motion from the initial position to the target with the left index fingertip (hand mirror-position matching). Fig. 2A demonstrates the corresponding targets for the left, matching, arm as mirror images of the right, reference, arm targets. For

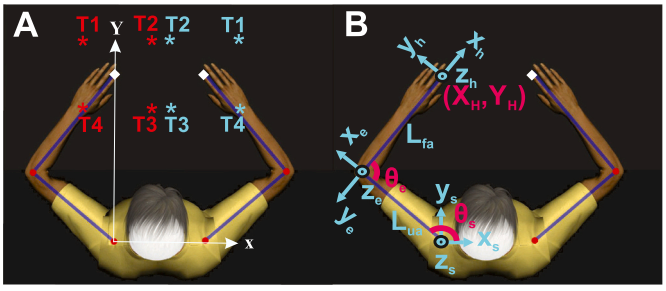

Fig. 2. Schematic of experimental setup and geometric arm model. A: Bimanual hand mirror-position matching experiment. The initial positions of the left and right index fingertips are marked as white diamonds. Red and cyan colored asterisks are the four targets for each arm (T1, T2, T3 and T4). Cyan asterisks indicate targets to which the robot moved the right hand; red asterisks correspond to the mirror images of the cyan asterisks and indicate the targets reached by the subject with the left hand to match the corresponding right targets. B: Coordinates of arm joints and parameters of the arm model for computing the forward kinematics using the Jacobian matrix (Eq. (4)). The origins of the shoulder, elbow and hand coordinate frames are at the shoulder, elbow and index fingertip, respectively. The positive directions of the corresponding x and y axes are indicated by the arrows; the direction of the z axes is perpendicular to the xy plane. θ_s and θ_e denote angles of the shoulder and elbow joints; L_{ua} and L_{fa} are the lengths of the upper arm and forearm+hand segments. (For interpretation of the references to color in this figure legend, the reader is referred to the web version of this article.)

Table 1
Characteristics of subjects.

Subject	Age, years	Sex	Height, cm	Forearm + hand length, cm	Upper arm length, cm
1	21	F	155	38.9	29.9
2	23	F	152	37.5	25.0
3	19	M	165	39.8	29.3
4	47	M	178	43.7	31.9
5	25	M	181	46.7	31.5
6	19	F	168	41.1	28.8
7	29	F	156	38.9	32.1
8	20	M	175	43.7	29.1
9	22	M	170	47.7	33.1
10	22	M	170	41.3	27.3
11	52	M	188	47.2	26.3
Mean	27.2	_	168.9	42.41	29.48
SD	11.4		11.4	3.62	2.56

example, when the right index fingertip was moved to target T2 (cyan T2 target in Fig. 2A), the subject would match this right-hand position by moving the left index fingertip in the mirror direction by the same distance (red T2 target in Fig. 2A). Note that for a two-joint arm in the horizontal plane, there is a one-to-one correspondence between the two joint angles and the corresponding two Cartesian coordinates of the hand. To account for differences in the subjects' arm length, the target distance for each subject (D_T) was normalized based on the distance between the hand (the index finger tip) and shoulder at the initial hand position:

$$D_T = 14.14\left(\frac{x}{50.7}\right) \quad (1)$$

In the equation, x is the distance in cm between the index fingertip initial position and the shoulder of a given subject; 50.7 is the same distance in cm for the subject from a preliminary study whose forearm+hand length and upper arm lengths were 40.86 cm and 30.01 cm, respectively. For that subject the distance to the targets from the initial position was 14.14 cm with targets located at the corners of a 20-cm x 20-cm square. Because of this normalization, the absolute target distances from the initial hand position for all subjects ranged from 11.5 cm to 16.6 cm.

When the right index fingertip moved by the robot reached a target and stopped, the Kinarm generated a 200-ms beeping sound, indicating that the subject could start moving the left arm to perform hand mirror-position matching. The assigned time for performing the matching task was 2.5 s. The subjects were instructed to hold the position of the left hand when they reached the matching mirror position until the Kinarm moved both arms back to the initial positions. Hand mirror-position matching was repeated 72 times (18 times for each target) with a 5-min break after every 24 repetitions. During the experiment, the targets and arms were hidden from the subject's view by a non-transparent screen and cloth.

2.1.3. Analysis of experimental data

To evaluate the precision (random errors) of the hand mirror-position matching, we analyzed position errors of the left, matching index fingertip with respect to the mirror position of the corresponding right, reference index fingertip, which were recorded in each trial. Random errors at each target of each subject were obtained by subtracting the mean coordinates of the left hand along the left-right and backward-forward axes obtained across 18 trials for each target and subject from the left-hand coordinates recorded in each trial. The obtained differences represented random errors of arm mirror-position matching for a given target and subject. The experimental distribution of these errors was fitted by the tolerance ellipse (Johnson & Wichern, 2007).

Each ellipse was characterized by 3 independent parameters: the direction of the major axis, size (area), and elongation (shape), i.e., the ratio of the lengths of the major and minor axes. The ellipse direction was defined as the angle between the ellipse major axis and the left-right axis and had a range of 0^o – 90^o. The positive and negative orientation angles corresponded to the counterclockwise and clockwise rotations of the major axis from the left-right axis, respectively.

To compare the results of our experiments with the literature, e.g. (Haggard, Newman, Blundell, & Andrew, 2000; Rincon-Gonzalez et al., 2011; Rossetti et al., 1994; Slinger & Horsley, 1906; von Hofsten & Rosblad, 1988; Wilson et al., 2010), we also computed the mean of the absolute values of the radial and azimuth random hand mirror-position errors from the projections of random errors on the line connecting the left shoulder and the left hand and on the line perpendicular to the shoulder-hand line, respectively, for each subject across all targets, and for distant targets (T1 and T2) and close targets (T3 and T4; Fig. 2A). Similarly, we computed the mean of the absolute values of backward-forward and left-right random errors from the projections of random errors on the forward-backward and left-right axes, respectively.

2.2. Geometric analysis of transformation from joint position errors to hand position errors

We conducted a Jacobian-based geometric analysis of a planar, two-joint kinematic chain representing the human arm (Fig. 2B). In this geometric model, the relationship between the hand position $(X_H, Y_H)^T$ and the joint angles at the shoulder and the elbow (θ_s, θ_e) could be expressed as follows:

$$\begin{bmatrix} X_H \\ Y_H \end{bmatrix} = f(\theta_s, \theta_e) = \begin{bmatrix} f_x(\theta_s, \theta_e) \\ f_y(\theta_s, \theta_e) \end{bmatrix} \tag{2}$$

where $f(\theta_s, \theta_e)$ is a forward kinematic transformation function that was computed using the four Denavit-Hartenberg parameters (Denavit & Hartenberg, 1955; Spong & Vidyasagar, 1989).

If the shoulder coordinate frame is set as shown in Fig. 2B (Z axis is perpendicular to the XY plane), the transformation from the shoulder coordinates to the hand coordinates $T(\theta_s, \theta_e)$ can be represented as the product of several rotation (Rot) and translation (Trans) matrices:

$$T(\theta_s, \theta_e) = Rot(Z_s, \theta_s)Trans(X_s, L_{ua})Rot(Z_e, -\pi + \theta_e)Trans\left(X_e, L_{fa}\right) =$$

$$\begin{bmatrix} cos(\theta_s) & -sin(\theta_s) & 0 & 0 \\ sin(\theta_s) & cos(\theta_s) & 0 & 0 \\ 0 & 0 & 1 & 0 \\ 0 & 0 & 0 & 1 \end{bmatrix} \begin{bmatrix} 1 & 0 & 0 & L_{ua} \\ 0 & 1 & 0 & 0 \\ 0 & 0 & 1 & 0 \\ 0 & 0 & 0 & 1 \end{bmatrix} \begin{bmatrix} cos(-\pi + \theta_e) & -sin(-\pi + \theta_e) & 0 & 0 \\ sin(-\pi + \theta_e) & cos(-\pi + \theta_e) & 0 & 0 \\ 0 & 0 & 1 & 0 \\ 0 & 0 & 0 & 1 \end{bmatrix} \begin{bmatrix} 1 & 0 & 0 & L_{fa} \\ 0 & 1 & 0 & 0 \\ 0 & 0 & 1 & 0 \\ 0 & 0 & 0 & 1 \end{bmatrix} \tag{3}$$

where X_s and Z_s are the axes of the shoulder coordinate frame; X_e and Z_e are the axes of the elbow coordinate frame; and L_{ua} and L_{fa} denote the length of the upper arm and forearm with hand. In the 4 × 4-matrix $T(\theta_s, \theta_e)$, the first three elements of the fourth column are the x, y, and z coordinates of the hand position expressed as functions of the shoulder and elbow angles. Therefore, the position of the hand in the horizontal workspace can be expressed as:

$$\begin{bmatrix} X_H \\ Y_H \end{bmatrix} = \begin{bmatrix} f_x(\theta_s, \theta_e) \\ f_y(\theta_s, \theta_e) \end{bmatrix} = \begin{bmatrix} T(\theta_s, \theta_e)_{(1,4)} \\ T(\theta_s, \theta_e)_{(2,4)} \end{bmatrix} =$$

$$= \begin{bmatrix} L_{fa}cos(\theta_s)cos(-\pi + \theta_e) - L_{fa}sin(\theta_s)sin(-\pi + \theta_e) + L_{ua}cos(\theta_s) \\ L_{fa}sin(\theta_s)cos(-\pi + \theta_e) + L_{fa}cos(\theta_s)sin(-\pi + \theta_e) + L_{ua}sin(\theta_s) \end{bmatrix} \tag{4}$$

From Eq. (4), one can derive the relationship between small changes in joint angles $(\Delta\theta_s, \Delta\theta_e)^T$and the corresponding changes in hand position $(\Delta X_H, \Delta Y_H)^T$:

$$\begin{bmatrix} \Delta X_H \\ \Delta Y_H \end{bmatrix} = \boldsymbol{J} \begin{bmatrix} \Delta\theta_s \\ \Delta\theta_e \end{bmatrix} \tag{5a}$$

$$\begin{bmatrix} \Delta\theta_s \\ \Delta\theta_e \end{bmatrix} = \boldsymbol{J}^{-1} \begin{bmatrix} \Delta X_H \\ \Delta Y_H \end{bmatrix} \tag{5b}$$

where $\boldsymbol{J}$ is the Jacobian matrix:

$$\boldsymbol{J} = \begin{bmatrix} \frac{\partial f_x}{\partial \theta_s} & \frac{\partial f_x}{\partial \theta_e} \\ \frac{\partial f_y}{\partial \theta_s} & \frac{\partial f_y}{\partial \theta_e} \end{bmatrix} \tag{6}$$

The changes in hand position caused by small changes in shoulder and elbow angles can be quantified by singular values of $\boldsymbol{J}$, which are the square roots of eigenvalues of $\boldsymbol{J}^*\boldsymbol{J}$, where $\boldsymbol{J}^*$ is the conjugate transpose of $\boldsymbol{J}$; e.g., (Bretscher, 2013). For example, the maximum singular value of $\boldsymbol{J}$, or the Euclidean norm of $\boldsymbol{J}$, is the maximum change that occurs in the hand position given small changes in the joint angles (see Eq. (5a)):

$$\|\boldsymbol{J}\| = max_{i=1,n}\sqrt{\lambda_i(\boldsymbol{J}^*\boldsymbol{J})} \tag{7}$$

where $\lambda_i(\boldsymbol{J}^*\boldsymbol{J})$ is the i-th eigenvalue of $\boldsymbol{J}^*\boldsymbol{J}$ and n is the rank of $\boldsymbol{J}$. In other words, the Euclidean norm of the Jacobian matrix provides the measure of the maximum displacement of the hand caused by the combination of small angular displacements at the shoulder and elbow within a unit circle:

$$\sqrt{\Delta\theta_s^2 + \Delta\theta_e^2} < 1 \tag{8}$$

Similarly, the minimum hand displacement caused by small joint angle changes is determined as the square root of the minimum eigenvalue of $\boldsymbol{J}^*\boldsymbol{J}$ (Bretscher, 2013). In addition, eigenvectors $\boldsymbol{\nu}$ satisfying (9) were computed for given arm configurations. The eigenvectors corresponding to the maximum and minimum eigenvalues indicate the directions of the maximum and minimum displacements of the hand for a given input of small joint angle deviations $(\Delta\theta_s, \Delta\theta_e)^T$:

$$\boldsymbol{J}^*\boldsymbol{J}\boldsymbol{\nu} = \lambda\boldsymbol{\nu} \tag{9}$$

The computed eigenvectors were multiplied by $\boldsymbol{J}$, so that they expressed the directions of small displacements in the hand

coordinates (Bretscher, 2013). The eigenvalues and eigenvectors were used to construct a precision ellipse of hand position with the center at the left-hand location (X_H, Y_H). The length and direction of the semi-major axis of the ellipse corresponded to the maximum singular value of $\boldsymbol{J}$ and $\boldsymbol{J}\nu_{max}$, respectively (ν_{max} is the eigenvector of the maximum eigenvalue). The length and direction of the semi-minor axis corresponded to the minimum singular value of $\boldsymbol{J}$ and $\boldsymbol{J}\nu_{min}$, respectively (ν_{min} is the eigenvector of the minimum eigenvalue). With these ellipse parameters, precision ellipses were plotted for given arm configurations using Matlab function *ellipse1* (Matlab R2016a, MathWorks Inc., Natick, MA, USA).

Another geometric parameter characterizing the relationship between small changes in joint angles and the corresponding changes in hand position (see Eq. (5a)) is the condition number $\kappa(\boldsymbol{J})$, i.e., the square root of the ratio between the maximum and minimum eigenvalues of $\boldsymbol{J}^*\boldsymbol{J}$. The condition number can be thought of as an error amplification factor since it reflects how errors in the joint angle space induce errors in the hand position (Merlet, 2006):

$$\kappa(\boldsymbol{J}) = \|\boldsymbol{J}\|\left\|\boldsymbol{J}^{-1}\right\| \tag{10}$$

Since the condition number is defined as the ratio of the lengths of the major and minor axes of the precision ellipse, condition numbers that differ from a value of one indicate that there is a preferred error direction at a given arm posture, as opposed to equal errors in all directions.

To derive hand precision ellipses corresponding to physiologically relevant random angle errors at the shoulder and elbow, $(e_s, e_e)^T$, a modified Jacobian matrix was used:

$$\boldsymbol{J}_m = \boldsymbol{J}\begin{bmatrix} e_s & 0 \\ 0 & e_e \end{bmatrix} \tag{11}$$

This matrix scales joint angle errors and changes the unit circle input in the space of joint angle errors (see Eq. (8)) into an elliptical input:

$$\sqrt{\frac{\Delta\theta_s^2}{e_s^2} + \frac{\Delta\theta_e^2}{e_e^2}} < 1 \tag{12}$$

The deviations in the joint angle space in Eq. (12), $(\Delta\theta_s, \Delta\theta_e)^T$, can be thought of as the precision (random errors) of joint angle position sense within the detection thresholds $(e_s, e_e)^T$. The detection threshold has been shown to depend on the joint, the imposed joint rotation speed, and whether the joint movement is passive or active, i.e., imposed on the joint by external forces or produced voluntarily (Hall & McCloskey, 1983). Hall and McCloskey (1983) measured detection thresholds for imposed rotations of elbow and shoulder joints as a function of the angular speed between 0.156 °/s and 80 °/s. Since our hand mirror-position matching tasks were static (see above), we estimated the shoulder and elbow detection thresholds at zero angular speed by extrapolating the data from Hall and McCloskey using least-squares fit regressions:

$$e_s^{HM} = 3.0145 \cdot e^{-4.8969 \cdot \dot{\theta}_s} + 0.1245 \tag{13a}$$

$$e_e^{HM} = 3.8299 \cdot e^{-4.5809 \cdot \dot{\theta}_e} + 0.1414 \tag{13b}$$

where $\dot{\theta}_s$ and $\dot{\theta}_e$ are shoulder and elbow angular speeds in °/s. The computed angle detection thresholds for the shoulder and elbow at zero speed were e_s^{HM}=3.14° and e_e^{HM} = 3.97°, respectively (Table 2). These values were used as the limits of random joint errors in the derivations and plotting of the hand precision ellipses for a single arm (see Eqs. (5a), (11), and (12)).

To compare predicted precision ellipses with ellipses obtained in the hand mirror-position matching experiment (see above), we considered that joint position errors in the matching arm should also depend on joint position errors in the reference arm (Cohen, 1958; Hakuta et al., 2014; Lackner, 1984; Simani, McGuire, & Sabes, 2007; von Hofsten & Rosblad, 1988). Since we do not know how perceived joint angles in the two arms are processed and combined by the brain, we computed two sets of random errors (standard deviations) of perceived angular positions at shoulder and elbow of the matching arm with two assumptions. These assumptions corresponded to the most precise (Model 1) and the least precise (Model 2) evaluation of matching arm joint positions, respectively. The actual precision of the matching arm joint positions should be somewhere between these two extremes. For the first set of joint errors (Model 1), we assumed that joint angular positions of the reference and matching arm are perceived simultaneously (in parallel). In this case the variance of a perceived joint position in the matching arm should be equal to the sum of the reciprocals of the

Table 2
Estimated random errors at shoulder (e_s) and elbow (e_e) of matching arm.

Derivation method / assumption	e_s, deg	e_e, deg
Extrapolation to zero joint velocity from experimentally obtained relationships between joint motion perceptual threshold and joint velocity (Hall & McCloskey, 1983) for a single arm (Eqs. (13a), (13b)): e_s^{HM} and e_e^{HM}	3.14	3.97
Simultaneous (in parallel) perception of joint angular positions in the reference and matching arm (Eqs. (14a), (14b); Model 1): e_s^{par} and e_e^{par}	2.22	2.80
Independent (in series) perception of joint angular positions in the reference and matching arm (Eq. (15a), (15b); Model 2): e_s^{ser} and e_e^{ser}	4.44	5.62
Computed from experimental precision ellipses (see Eq. (5b)) of each subject and 4 targets and averaged (mean ± SD); Model 3	3.45 ± 0.97	4.41 ± 1.18

corresponding variances of the perceived joint position in the two arms, e.g. (Howard, 1997; van Beers, Sittig, & Denier van der Gon, 1996). This estimate gives the smallest variance (Maybeck, 1979). Thus, assuming the same precision of joint angular position estimation in the two arms, the corresponding standard deviations of perceived joint position at shoulder (e_s^{par}) and elbow (e_e^{par}) of the matching arm were computed as (Howard, 1997; Maybeck, 1979; van Beers et al., 1996):

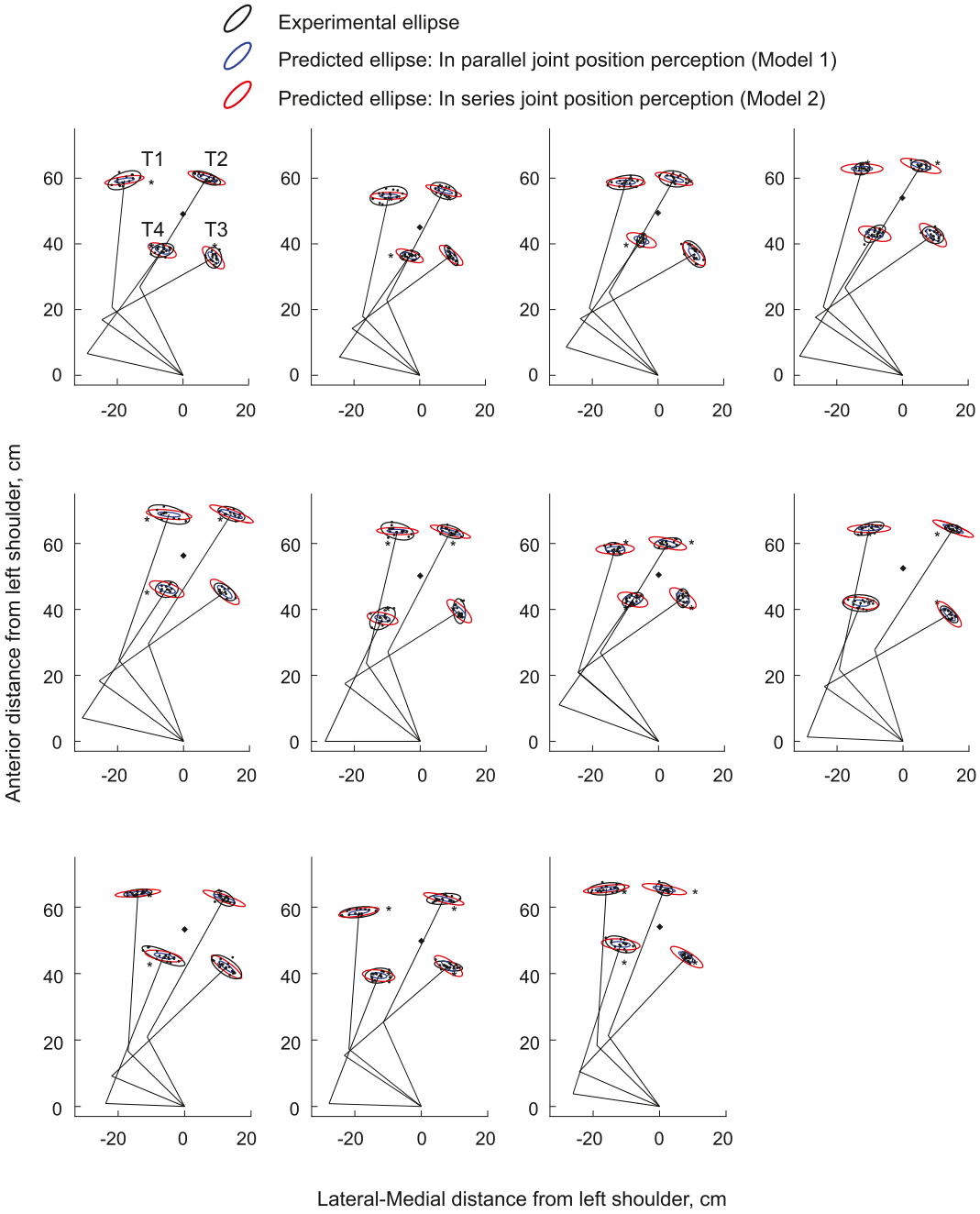

Fig. 3. Measured (black lines) and predicted by the model (blue and red lines) hand precision ellipses for four targets of all subjects. Small black circles demonstrate results of multiple trials. The upper arm and forearm+hand are displayed as black lines. The black asterisks indicate target positions (T1, T2, T3, and T4); the black diamonds denote the initial hand position. The endpoint of the arm at each posture coincides with the mean hand position across multiple trials. For display purposes, the location of actual data and targets, arm segments lengths, and the distance from the left shoulder to the initial point of each subject were scaled so that all targets were at a distance of 10 cm from the initial point. To reduce clatter, only predicted ellipses by Models 1 and 2 are shown; ellipses predicted by Model 3 have the same orientations; the length of the major and minor axes of ellipses predicted by Mode3 is between those of Models 1 and 2. (For interpretation of the references to color in this figure legend, the reader is referred to the web version of this article.)

$$e_s^{par} = \sqrt{\frac{\left(e_{s\_ref}^{HM}\right)^2 \cdot \left(e_{s\_match}^{HM}\right)^2}{\left(e_{s\_ref}^{HM}\right)^2 + \left(e_{s\_match}^{HM}\right)^2}} = \frac{e_s^{HM}}{\sqrt{2}} \tag{14a}$$

$$e_e^{par} = \sqrt{\frac{\left(e_{e\_ref}^{HM}\right)^2 \cdot \left(e_{e\_match}^{HM}\right)^2}{\left(e_{e\_ref}^{HM}\right)^2 + \left(e_{e\_match}^{HM}\right)^2}} = \frac{e_e^{HM}}{\sqrt{2}} \tag{14b}$$

where $e_{s\_ref}^{HM} = e_{s\_match}^{HM} = e_s^{HM}$ correspond to the standard deviation of perceived shoulder position in the reference and matching arm, estimated from the study of Hall and McCloskey (1983) (see above); $e_{e\_ref}^{HM} = e_{e\_match}^{HM} = e_e^{HM}$ correspond to the standard deviation of perceived elbow position in the reference and matching arm, estimated from the study of Hall and McCloskey (1983).

To compute the second set of standard deviations of perceived joint positions in the matching arm (Model 2), we assumed that joint angular positions of the reference and matching arm are perceived independently (in series), in which case the variances of perceived joint positions in the two arms should be added, e.g. (Howard, 1997; Maybeck, 1979; van Beers et al., 1996). This estimate gives the largest variance. The corresponding standard deviations of perceived joint positions at shoulder (e_s^{ser}) and elbow (e_e^{ser}) of the matching arm were computed as:

$$e_s^{ser} = \sqrt{\left(e_{s\_ref}^{HM}\right)^2 + \left(e_{s\_match}^{HM}\right)^2} = \sqrt{2} \cdot e_s^{HM} \tag{15a}$$

$$e_e^{ser} = \sqrt{\left(e_{e\_ref}^{HM}\right)^2 + \left(e_{e\_match}^{HM}\right)^2} = \sqrt{2} \cdot e_e^{HM} \tag{15b}$$

We also computed standard deviations of perceived shoulder and elbow positions in the matching arm from experimental hand precision ellipses (see Eq. (5b)) for each subject and target and then averaged them (Model 3), see Table 2. These estimates corresponded to the assumption that hand precision depends exclusively on the random joint errors and the joint-to-hand coordinate transformation.

2.3. Statistical analysis

We used a repeated measures ANOVA (IBM SPSS v21 software; Chicago, IL, USA) to test if precision of hand position sense was the same (uniform) at 4 different locations of the hand in the horizontal plane. We determined the effect of Target location (independent factor) on the parameters of the hand precision ellipses (dependent variables) – precision ellipse orientation, area, and shape. We also tested if parameters of predicted hand precision ellipses were closely related to the ellipse parameters obtained experimentally for each subject and target by computing the Pearson correlation coefficient between the predicted and measured ellipse parameters. We performed this correlation analysis for predictions obtained for each of 3 sets of estimated random joint errors (Table 2, Models 1–3). In addition, we compared the mean random errors between the radial and azimuth directions, backward-forward and left-right directions, and between distant (T1 and T2) and close (T3 and T4) targets for the experimental data and model predictions. A two-way repeated measures ANOVA with two independent factors of Method (Experiment and Model) and Target Distance was performed for each dependent variable (the mean random error computed for specific conditions). The Games-Howell test with Bonferroni adjustments was used for pairwise comparisons. Descriptive statistics values are reported as the mean ± standard deviation (SD). The significance level for all tests was set at an alpha level of 0.05.

3. Results

3.1. Precision of arm position sense in hand mirror-position matching

The hand precision ellipses obtained experimentally for each subject demonstrated target specific orientations ($F(3,240) = 27.5$, $p < 0.001$; Fig. 3, black ellipses). For example, ellipses at the right targets T2 and T3 typically had a negative orientation angle that was greater for T3 ($-46.6^o \pm 31.3^o$) than for T2 ($-12.6^o \pm 12.2^o$); $p < 0.001$). The ellipses at the left targets were either nearly parallel to the lateral-medial axis (T1: $4.0^o \pm 12.8^o$) or had the opposite orientation (T4: $13.5^o \pm 26.7^o$). Ellipse orientations at these targets were not statistically different ($p = 1.0$); ellipse orientations at T1 and T2 were not different ($p = 0.122$) and the orientation at T4 was different from that of T2 and T3 ($p < 0.002$). The experimentally determined ellipse size (area) and shape were not affected by the target position ($F(3,240 = 0.725$, $p = 0.538$ and $F(3, 240) = 0.860$, $p = 0.462$, respectively). The ellipse areas ranged from 29.1 $cm^2 \pm$ 11.7 cm^2 to 41.1 $cm^2 \pm$ 19.6 cm^2 and ellipse shapes (condition numbers, Eq. (10)) ranged from 2.0 ± 0.69 to 2.5 ± 0.78.

To further quantify non-uniform precision of hand position sense in hand mirror-position matching, we computed the mean absolute random errors in the radial and azimuth, backward-forward and left-right directions for distant (T1 and T2) and close (T3 and T4) targets (see Methods). A repeated measures ANOVA revealed that the mean random error in the azimuth direction was greater at distant targets than at close targets (4.50 ± 1.33 cm vs 3.53 ± 1.12 cm, $F(1,21) = 6.5$, $p = 0.019$; Fig. 4A1, Experiment). Similar results were obtained for the random errors in the left-right direction; the mean random error was greater at distant targets than at close ones

(4.50 ± 1.13 cm vs 3.47 ± 1.33 cm, F(1,21) = 13.1, $p = 0.002$); Fig. 4A3, Experiment).

The mean error in the radial direction had a tendency to be smaller at distant targets compared to the close targets but the difference did not reach the significance level (2.93 ± 1.07 cm vs 3.41 ± 0.89 cm, F(1,21) = 3.4, $p = 0.080$); Fig. 4A2, Experiment. Similar results were obtained for the mean random error in the backward-forward direction, although in this case the difference in random errors between distant and close targets reached significance level (2.26 ± 0.50 cm vs 2.70 ± 0.71 cm, F(1, 21) = 6.2 $p =$ 0.021; Fig. 4A4, Experiment).

The comparison between the mean precision errors in the azimuth and radial directions across all targets revealed that the azimuth random error was greater (4.02 ± 1.31 cm vs 3.17 ± 1.00 cm, F(1,43) = 14.7, $p < 0.001$; Fig. 4B1, Experiment. Similarly, the random

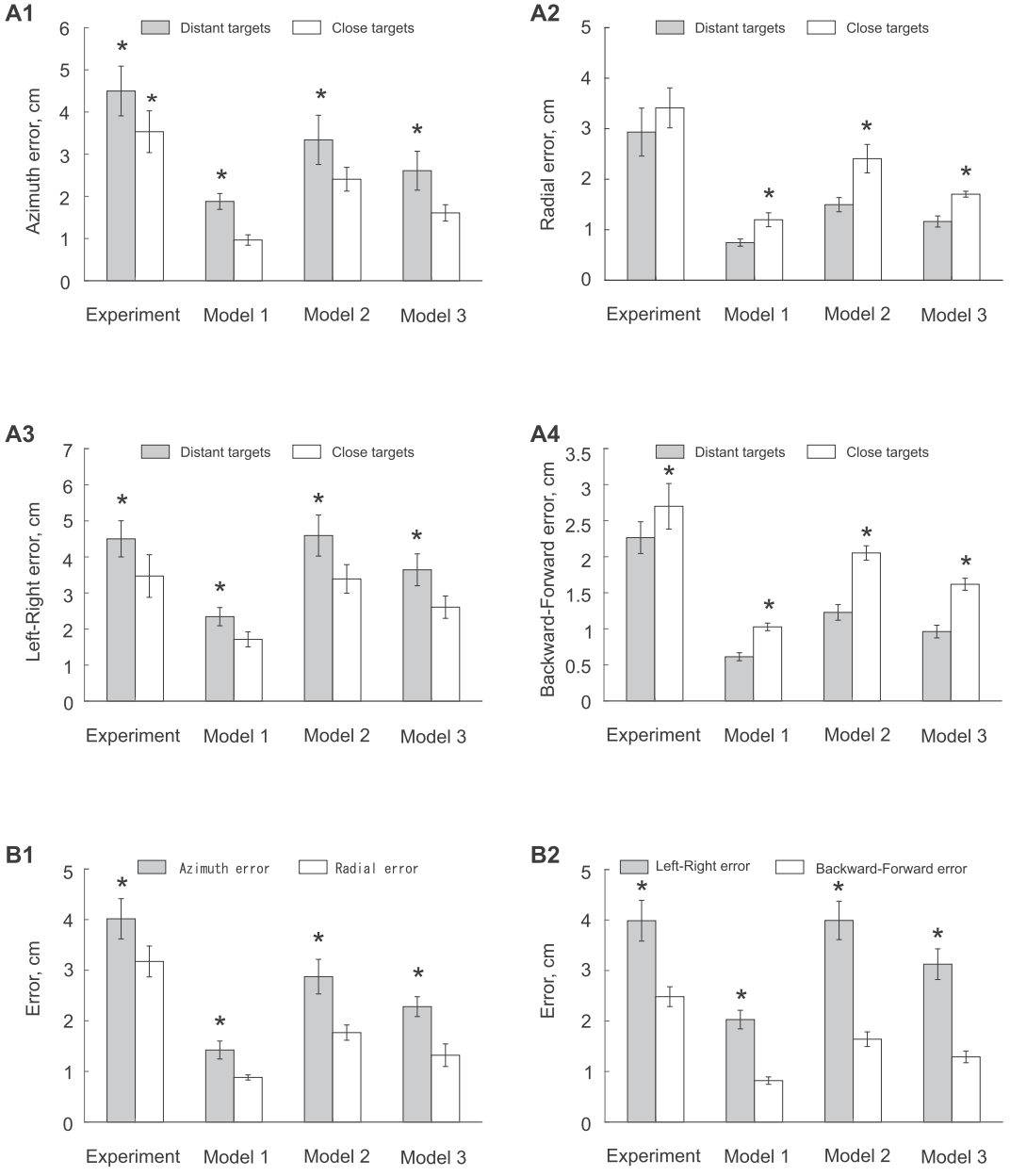

Fig. 4. Comparisons of measured and predicted by the model mean random errors in different directions for distant (T1 and T2) and close (T3 and T4) targets (Fig. 2A); mean ± SD. Asterisks indicate statistical difference between targets and types of error ($p < 0.05$). Models 1 and 2 correspond to in parallel and in series perception of joint positions in the reference and matching arm; in Model 3, random errors at the shoulder and elbow were computed from experimental precision ellipses (see Table 2). A1: Azimuth random errors for distant and close targets. A2: Radial random errors for distant and close targets. A3: Random errors in the right-left direction for distant and close targets. A4: Random errors in the backward-forward direction for distant and close targets. B1: Comparison of random errors between Azimuth and Radial directions across all targets. B2: Comparison of random errors between left-right and forward-backward directions across all targets.

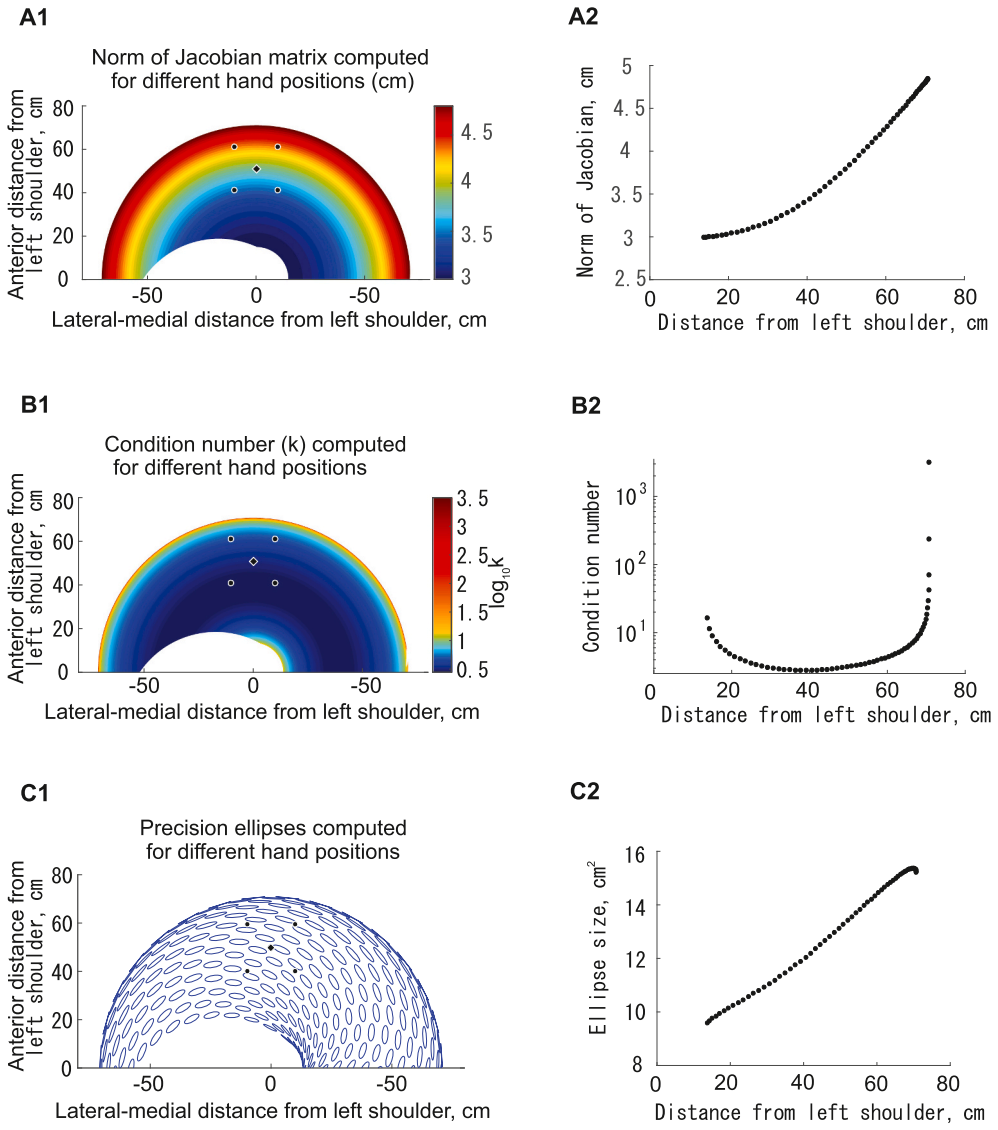

Fig. 5. Results of geometric analysis of the transformation of random joint angle errors to random errors of hand position in a two-segment arm model. Arm segment lengths were set at L_{ua} = 30.01 cm and L_{fa} = 40.86 cm, where L_{ua} is the upper arm length and L_{fa} is the forearm+hand length. The random errors at shoulder and elbow were set at 3.14° and 3.97°, respectively; Table 1. In all left panels, the black circles indicate four target positions for the left arm (Fig. 2A); the black diamond is the initial position of the left index fingertip. A1: Color map of the norm of Jacobian matrix (or maximum random error) (Eq. (7)) in the horizontal workspace within the reach of the index fingertip. The coordinates (0,0) correspond to the location of the left shoulder. The norm was computed and plotted for arm configurations corresponding to the elbow and shoulder angles in the ranges of 0.1–3.14 and 0.1–4.08 rad, respectively, with a step of 0.2 rad. The white region in the vicinity of the shoulder indicates the region that could not be reached by the left index fingertip. A2: The Jacobian norm as a function of the distance between the index fingertip and shoulder. B1: Color map of the condition number (ratio of lengths of the major and minor axes of precision ellipse) in the horizontal workspace in logarithmic scale. B2: The condition number as a function of the distance between the index fingertip and shoulder. C1: Precision ellipses computed for different hand locations in the horizontal workspace assuming the perception thresholds of 3.14° and 3.97° for the shoulder and elbow joints (see text and Table 2 for details). The center of each ellipse coincides with the corresponding index fingertip location. The ellipses were plotted in the ranges of 0.1–3.14 and 0.1–4.08 rad for elbow and shoulder joints, respectively, with a step of 0.2 rad. C2: Ellipse size (area) as a function of the distance between the index fingertip and shoulder.

errors in the left-right direction were greater than those in the backward-forward direction (3.99 ± 1.33 cm vs 2.48 ± 0.65 cm, F(1, 43) = 45.4, p < 0.001; Fig. 4B2, Experiment).

3.2. Effects of joint-to-hand coordinate transformation on hand position precision

3.2.1. Geometric analysis of hand position precision

The results of Jacobian-based geometric analysis revealed how the transformation of random errors in joint coordinates to random errors in external hand coordinates contributed to the non-uniform distribution of random errors in hand position. We evaluated the distribution of random errors of hand position using parameters of the hand precision ellipse. For this geometric analysis we used joint random errors estimated from (Hall & McCloskey, 1983) (Table 2, e_s^{HM} and e_e^{HM}). The computed maximum random error of the hand position, represented as the norm of the Jacobian matrix (Eq. (7)) and related to the length of the major axis of the precision ellipse, increased monotonically with the distance of the hand from the shoulder (Fig. 5A1, A2).

The condition number, indicating the precision ellipse shape and presence of a preferred error direction (Eq. (10)), was close to 2 at an intermediate distance from the body (between approximately 30 and 50 cm), whereas it was relatively high in the vicinity of the body (~15 cm), and extremely high in the most distant region where the arm was close to full extension (Fig. 5B1, B2).

The orientation and shape of the precision ellipses varied with the hand position in the horizontal workspace (Fig. 5C1). The major axis of the ellipses was oriented almost parallel to the backward-forward axis at extreme left and right hand positions, and nearly parallel to the lateral-medial axis for hand positions of ~0–25 cm to the left of the shoulder and farther than ~20 cm in front of the shoulder.

The size (area) of the precision ellipses also varied with the hand position. The ellipse area increased as a linear function of the distance from the shoulder except at the most distant hand position (Fig. 5C2).

3.2.2. Random errors at shoulder and elbow of the matching arm

The random errors of shoulder and elbow angular positions in the geometric model of the matching arm depended on our assumptions of how perceived joint positions of the reference and matching arms are processed and combined. The assumption that joint positions of the two arms were perceived simultaneously (in parallel) gave the following random errors: $e_s^{par} = 2.22^o$ and $e_e^{par} = 2.80^o$ (Table 2, Model 1). The assumption of independent (in series) perception of shoulder and elbow joint position of the two arms resulted in higher estimates of random errors: $e_s^{ser} = 4.44^o$ and $e_e^{ser} = 5.62^o$ (Table 2, Model 2). The random shoulder and elbow joint errors computed from the mean hand precision ellipse obtained experimentally (see above) using Eq. (5b) ($3.45^o \pm 0.97^o$ and $4.41^o \pm 1.18^o$, respectively; Table 2, Model 3) were in the middle of the range of the minimum and maximum errors of Model 1 and 2 and close to the errors derived from the data of Hall and McCloskey (Hall & McCloskey, 1983), i.e. $e_s^{HM} = 3.14^o$ and $e_e^{HM} = 3.97^o$. Note that in all estimates, the random errors were greater at the elbow than at the shoulder.

3.2.3. Comparison between predicted and experimental random errors of hand position sense

The predicted hand precision ellipses assuming in parallel (Model 1) and in series (Model 2) processing of perceived joint angles of the reference and matching arms (Fig. 3, blue and red ellipses, respectively) were qualitatively similar to the experimental precision ellipses (Fig. 3, black ellipses). Note that ellipses predicted by Model 2 were approximately 2 times longer and wider than those of Model 1; the major and minor axes of ellipses predicted by both models were parallel to each other. To quantitatively compare the predicted and experimental random errors of hand position sense in the radial and azimuth, backward-forward and left-right directions for distant (T1 and T2) and close (T3 and T4) targets, we applied a two-way repeated measures ANOVA with independent factors Method (Experiment and Model) and Target Distance (Distant and Close); see Methods.

The azimuth errors predicted by Models 1, 2 and 3 were greater at distant targets than at close ones (predicted error ranges: 1.88 cm – 3.34 cm vs 0.97 cm – 2.41 cm, $p < 0.001$, respectively), as was found experimentally (Fig. 4A1). However, the predicted errors were smaller than the experimental ones by 25–73%, p < 0.001). Similarly, the predicted left-right errors were greater at distant than at close targets (predicted error ranges: 2.34 cm – 4.59 cm vs 1.71 cm – 3.39 cm, p < 0.001, respectively), reproducing the experimental results (Fig. 4A3). There was no significant difference in the left-right errors between the experiment and predictions of Model 2 for both distant and close targets ($p = 1.0$), whereas predicted errors by Models 1 and 3 were significantly smaller (p < 0.001).

The predicted radial errors at distant targets were smaller than at close targets for all models (predicted error ranges: 0.75 cm – 1.50 cm vs 1.20 cm – 2.41 cm, respectively), the result that was similar to the experiment (Fig. 4A2). The experimental radial errors were greater than the errors predicted by all models, p < 0.001). Predicted errors in the backward-forward direction were likewise smaller at the distant than close targets for Models 1–3 (predicted error ranges: 0.61 cm – 1.23 cm vs 1.03 cm – 2.05 cm, p < 0.001, respectively), matching the experimental results (Fig. 4A4). The predicted errors for distant and close targets were significantly smaller than the corresponding experimental backward-forward errors (p < 0.001).

Comparisons between the predicted azimuth and radius errors across all targets revealed that the azimuth errors were larger for all models (predicted error ranges: 1.42 cm – 2.87 cm vs 0.88 cm – 1.77 cm, p < 0.001, respectively), matching the experimental results (Fig. 4B1). Similarly, the predicted left-right errors were greater than the predicted backward-forward errors (predicted error ranges: 2.03 cm – 3.99 cm vs 0.82–1.64 cm, $p < 0.001$, p < 0.001) in agreement with the experimental results (Fig. 4B2).

In summary, precision of hand position sense determined in bimanual hand mirror-position matching tasks and predicted by the arm geometric model and transformation from the joint to hand coordinates was non-uniform. Both measured and predicted azimuth and left-right precision was lower than radial and backward-forward precision, azimuth and left-right precision was greater at close targets, and radial and backward-forward precision was greater at distant targets.

3.2.4. Correlation between parameters of predicted and experimental precision ellipses

The Pearson correlation coefficients between parameters of the predicted and experimental precision ellipses (orientation, shape, and area) computed across all targets and subjects are shown in Table 3 and Fig. 6. The correlation coefficients between the predicted and experimental precision ellipse orientations were rather high and significant for all three Models of joint error estimations (r = 0.617–0.635, p < 0.001; Table 3). Correlation coefficients computed between the ellipse orientations predicted by the three models were close to 1.0 (r = 0.979–0.997, p < 0.001; Table 3; Fig. 3, Models 1 and 2). Scatter plots and linear regression lines for the experimental ellipse orientations and the orientations predicted by Models 1, 2 and 3 (Fig. 6A-C) demonstrated a greater range for the experimental orientation (between approximately -90° and + 70°) than for the predictions (between -50° and + 10°).

The next best predicted parameter of the precision ellipse was ellipse shape. The ellipse shape predicted by Model 2 correlated moderately with the experimental ellipse shape (r = 0.393, p = 0.008; Table 3). Correlation coefficients between the experimental ellipse shape and the predicted shape by Models 1 and 3 were low and insignificant (r = 0.200, p = 0.192 and r = 0.146, p = 0.346, respectively). Correlation coefficients computed between the ellipse shapes predicted by the three models were high and significant (r = 0.688–0.973, p = 0.001). The scatter plots and linear regression lines between the experimental ellipse shape and ellipse shape predicted by Models 1, 2 and 3 demonstrated a much greater range of values for the predictions (~ 2.5–12 for Models 1 and 3 and ~ 2.5–7 for Model 2) than for the experiment (between 1.1 and 4.0); see Fig. 6D-F.

The area of the hand precision ellipse was not well predicted by the arm geometric model. The Pearson correlation coefficients between the experimental and predicted ellipse areas were close to zero and not significant for Models 1, 2 and 3 (r = −0.038, p = 0.809; r = 0.068, p = 0.662; r = −0.075, p = 0.630; Table 3). Correlation coefficients computed between the ellipse areas predicted by Models 1 and 2 (r = 0.217, p = 0.157) and Models 2 and 3 (r = 0.129, p = 0.406) were insignificant, whereas predictions of Model 1 and 3 were highly correlated (r = 0.959, p < 0.001). The range of predicted ellipse areas by Models 1, 2 and 3 was much smaller (~ 3–36 cm^2) than the range of experimental areas (~ 10–75 cm^2; Fig. 6G-I).

In summary, despite qualitative similarities between predicted and experimental precision ellipses, such ellipse parameters as the ellipse shape and area were poorly predicted by the arm geometry and all three estimates of joint random errors (Models 1–3). Only the predicted ellipse orientation was significantly correlated with the experimental ellipse orientation.

4. Discussion

The goal of this study was to test the hypothesis that the non-uniform precision of hand position sense in a horizontal workspace results from the arm posture-related transformation of random errors of the arm joint positions to the hand position random errors. The random errors of hand position sense determined experimentally and predicted by a geometric analysis of the joint-to-hand position transformation demonstrated similar non-uniformities in the middle of the horizontal workspace. Specifically, random errors in the radial and forward-backward directions were smaller than in the azimuth and left-right directions and in locations closer to the body

Table 3
Pearson correlation coefficients between parameters of experimental and predicted precision ellipse.

Ellipse direction				
	Experiment	Model 1	Model 2	Model 3
Experiment	1	0.635*	0.617*	0.623*
Model 1		1	0.979*	0.997*
Model 2			1	0.985*
Model 3				1

Ellipse shape				
	Experiment	Model 1	Model 2	Model 3
Experiment	1	0.200	0.393*	0.146
Model 1		1	0.769*	0.973*
Model 2			1	0.688*
Model 3				1

Ellipse area				
	Experiment	Model 1	Model 2	Model 3
Experiment	1	−0.038	0.068	−0.075
Model 1		1	0.217	0.959*
Model 2			1	0.129
Model 3				1

Model 1, in parallel perception of joint angular positions in the reference and matching arm; Model 2, in series perception of joint angular positions in the reference and matching arm; Model 3, random joint angles computed from experimental precision ellipses; see Table 2. *, p < 0.001 (2-tailed tests after Fisher's z transformation, n = 44).

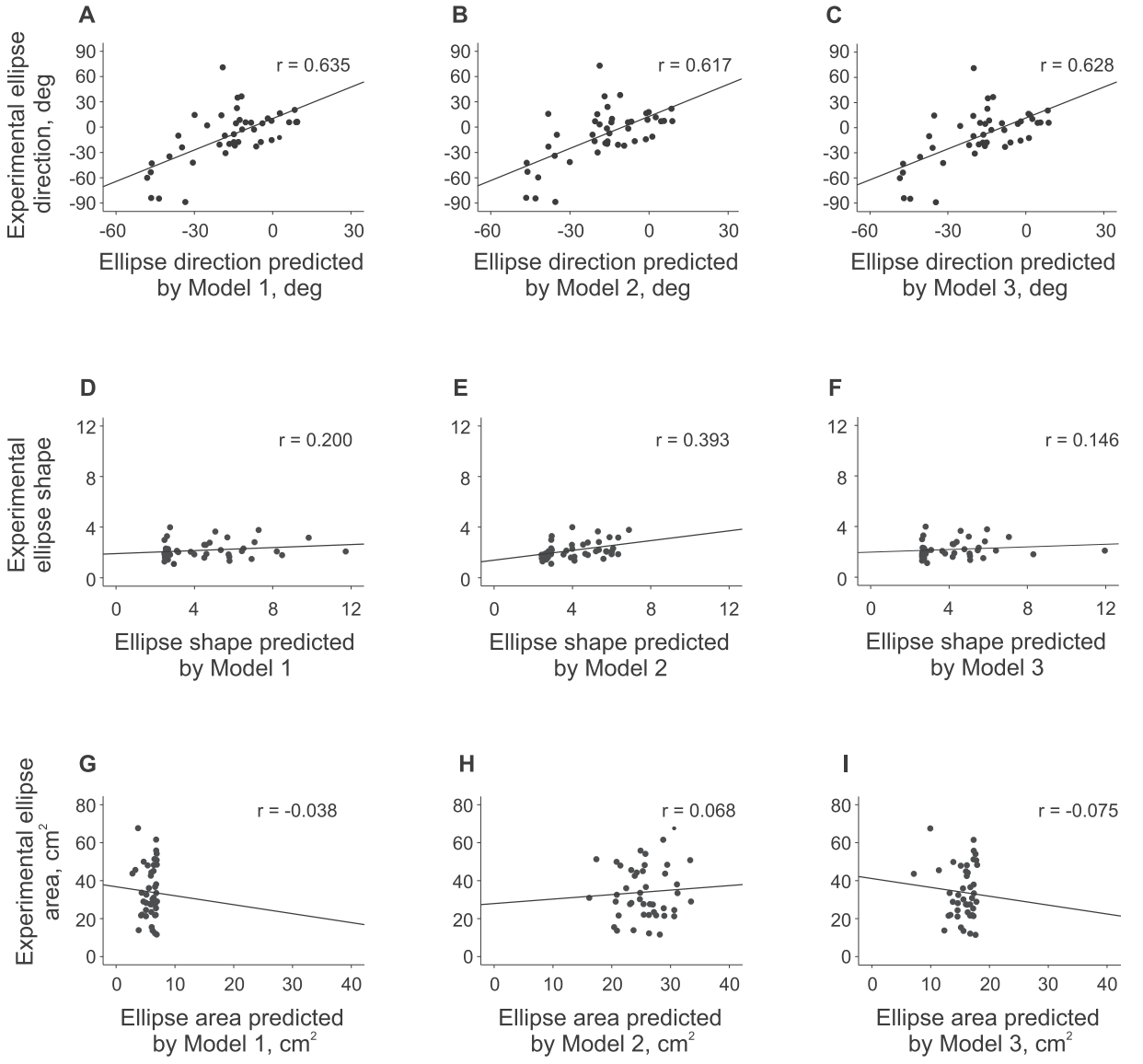

Fig. 6. Scatter plots and regression lines between predicted and experimental parameters of precision ellipses for all subjects and four targets. Predicted ellipses were computed using three sets of random errors at shoulder and elbow corresponding to Models 1, 2 and 3 (see Table 2). r is the Pearson correlation coefficient (see Table 3); $n = 44$. A, B and C: Scatter plots between experimental ellipse directions and ellipse directions predicted using Models 1, 2 and 3, respectively. D, E and F: Scatter plots between experimental ellipse shape and ellipse shape predicted using Models 1, 2 and 3, respectively. G, H and I: Scatter plots between experimental ellipse area and ellipse area predicted using Models 1, 2 and 3, respectively.

than further away, see Figs. 3 and 4. Our results on the non-uniform precision of hand position sense are in complete agreement with previous reports (Rincon-Gonzalez et al., 2011; Rossetti et al., 1994; Slinger & Horsley, 1906;van Beers et al., 1998; Wilson et al., 2010).

We also found that the experimentally obtained and predicted orientations of precision ellipses were highly correlated irrespective of the assumptions about how joint angular positions in the reference and matching arms are perceived (Table 3 and Fig. 6A-C). Note that Models 1, 2 and 3 did not predict the precision ellipse orientation with exactly the same accuracy (the correlation coefficients were slightly different: $r = 0.617$–0.635). A likely reason for these discrepancies is that we obtained numerical rather than analytical solutions of a nonlinear Eq. (9) to determine the orientation of the precision ellipse. On the other hand, correlations between the experimental and predicted ellipse shapes and areas were low, although the predicted ellipse shape was elongated (condition number $\kappa(\boldsymbol{J}) > 1$), in accordance with the experiment (Figs. 3, 5B2, C1, 6D-F). This suggests that the orientation of the precision ellipse and ellipse elongated shape, both predicted by the model, predominantly determine the non-uniform precision of the hand position sense reported in the literature and found in this study.

4.1. Transformation of random errors in joint coordinates to hand external coordinates explains the non-uniform precision of hand position sense in the horizontal workspace

The geometric arm model demonstrated an overall increase in the length of the major axis of the hand precision ellipse and in ellipse area with increasing distance from the shoulder to the hand (Fig. 5A1, A2, C2). This result is consistent with the decrease in the precision of hand position sense with increasing distance from the body reported in the literature (Rincon-Gonzalez et al., 2011; Rossetti et al., 1994; Slinger & Horsley, 1906; van Beers et al., 1998; Wilson et al., 2010) and experimentally found in this study for azimuth and left-right errors (Fig. 4A1, A3). However, the predicted and experimental ellipse areas did not demonstrate significant correlation (Table 3, Fig. 6G-I). This could be partially explained by the fact that only a small portion of the horizontal workspace was experimentally tested in this study and in this portion, the predicted ellipse area did not change substantially (Figs. 5C1 and 6G-I). The model also predicted and could explain the experimental fact that the precision of hand position sense is better in the radial and forward-backward directions than in the azimuth and right-left directions (van Beers et al., 1998; Wilson et al., 2010); also see the experimental results of this study (Fig. 4B1, B2). This fact is explained by the elongated shape and orientation of the precision ellipses in the azimuth direction in the middle of the horizontal workspace (Figs. 3 and 5C1). In the large workspace area lateral to the ipsilateral shoulder, in which the precision of hand position sense is often measured, the precision ellipses are oriented nearly parallel to the left-right axis (Fig. 5C1), explaining the greater precision in the backward-forward than in the left-right direction. Thus, our geometric model of the transformation of random errors at the shoulder and elbow angles to the hand position errors confirmed and generalized on the entire horizontal arm workspace previous conjectures about effects of arm geometric properties on precision of hand position sense (Scott & Loeb, 1994; van Beers et al., 1998; Wilson et al., 2010) obtained using less rigorous analysis (e.g., see Fig. 1).

As mentioned above, we tested precision of hand position sense in the small portion of the horizontal workspace. This, however, could not fully explain poor or no significant correlation between the experimental and predicted ellipse shape and area (Table 3, Fig. 6D-I), as well as substantial differences in precision ellipse size and shape (length of major and minor ellipse axes, ellipse area, and mean random errors) between the predictions and experiment; Figs. 3 and 4. These discrepancies could be expected if other factors besides the geometric arm properties affect the precision of hand position sense (see Introduction). One such factor could be the precision of angular position sense at the shoulder and elbow joints (see Eqs. (5a) and (12)). We derived these values for our model by first extrapolating thresholds of joint rotation detection measured for a single arm at different speeds to zero speed from the study of (Hall & McCloskey, 1983). We selected this indirect approach because of generally higher perceptual sensitivity to joint motion than to joint position in humans (Proske & Gandevia, 2018), because measurements of motion perception avoid drift in perception of position (Brown, Rosenbaum, & Sainburg, 2003; Clark, Larwood, Davis, & Deffenbacher, 1995), and because it reflects the distal-to-proximal gradient in precision of joint position sense (Hall & McCloskey, 1983). We then computed the largest and smallest precision of perceived joint positions in the matching arm assuming the same joint precision in the reference and matching arms and the in-parallel and in-series processing of the perceived joint positions in the two arms (Models 1 and 2, respectively). We also computed joint precision from the mean experimental hand precision ellipse (Model 3, Table 2).

Values of the precision of position sense at the shoulder and elbow measured more directly in unilateral or in bilateral joint angle matching experiments (Bevan, Cordo, Carlton, & Carlton, 1994; Darling, 1991; Fuentes & Bastian, 2010; Inglis, Frank, & Inglis, 1991; Lonn, Crenshaw, Djupsjobacka, & Johansson, 2000; Soechting, 1982; Soechting & Ross, 1984) are in the range of 3^o–9^o, after correcting for joint position perception in both reference and matching arms (Fuentes & Bastian, 2010; van Beers et al., 1998). Thus, all our estimates of the angular position precision at the shoulder and elbow, including those computed from the experimental hand precision ellipses (Model 3: 3.45^o and 4.41^o, respectively), are in the lower half or in the middle of the range of values reported in the literature. Given that our largest estimated random errors (Model 2: $e_s^{ser} = 4.44^o$ and $e_e^{ser} = 5.62^o$) exceed those determined from the experiment (Model 3), our estimates of joint precision cannot account for generally much smaller predicted random errors compared to the experimental ones (Fig. 4). A more likely reason for the smaller predicted errors and the lack of strong correlation between predicted and experimental precision ellipse shape and area (Fig. 6) is that there are additional sources of random errors in hand position sense. These additional sources are likely related to tonic muscle activity, coactivation of antagonists and the dependence of joint sensory thresholds on joint angles. Tonic muscle activity and antagonist coactivation are not normally measured in studies of joint and hand precision of position sense. Coactivation of antagonists, however, has been reported to improve precision of reaching movements; e.g. (Gribble, Mullin, Cothros, & Mattar, 2003). A relatively large range of joint position precision (3^o–9^o, see above) has been reported for different arm postures and joint angles. Thus, it is possible that joint position precision is joint angle-depended (e.g., Fuentes & Bastian, 2010). We did not consider the above factors in our model.

Other theoretical models of joint position acuity based on general assumptions about arm musculoskeletal properties and the distribution of muscle spindles across muscles (Scott & Loeb, 1994) or on assumptions about probability distributions of errors in proprioceptive and visual sources of hand location and the convolution of the distributions (van Beers et al., 1998) gave much lower uncertainty values of position sense at the shoulder and elbow (0.6^o-1.1^o). Using these estimates of joint random errors in our model would make the discrepancies between the model predictions and experimental results much larger.

Taken together, our results demonstrate that the transformation of uncertainties in joint angular positions to uncertainties in the hand position could explain the orientation and elongated shape of the hand precision ellipse and thus the non-uniform precision of hand position sense in the horizontal workspace. The precision ellipse shape and area predicted by the geometric model are not well correlated with the experimentally obtained ellipse shape and area.

4.2. Precision of hand position sense and arm stiffness

There is another property of the arm that strongly depends on the joint-to-hand coordinate transformation – arm stiffness, which can be characterized in the horizontal workspace by the arm stiffness ellipse. A theoretical arm stiffness ellipse can be computed from shoulder and elbow stiffnesses using a joint-to-hand Jacobian-based transformation similar to our model; see our Eqs. (5a) and (6) and (Flash & Mussa-Ivaldi, 1990; Hogan, 1985; Mussa-Ivaldi, Hogan, & Bizzi, 1985). Mussa-Ivaldi and colleagues (Mussa-Ivaldi et al., 1985) measured arm stiffness in human subjects and found that the orientation and shape of the stiffness ellipses were practically invariant over time, across subjects, and in different postural tasks for given arm postures, whereas the ellipse size varied. They also compared the experimental arm stiffness ellipses at different arm postures with the corresponding ellipses computed from constant joint stiffnesses obtained in the same experiment for a given arm posture. They concluded that arm posture had major effects on ellipse orientation and shape. Note that the procedure for comparing the experimental and computed arm stiffness ellipses and the obtained results closely resemble our comparison of the experimental and predicted by Model 3 precision ellipses and obtained results (Table 3). Subsequent studies have demonstrated a strong link between the measured arm stiffness ellipse and the hand precision ellipse in reaching and postural tasks with spatial accuracy requirements. Specifically, it has been shown that the major axes of the two ellipses are essentially orthogonal to each other and people can modify the orientation and area of the stiffness ellipse to improve performance of pointing or postural tasks (Franklin et al., 2007; Frolov, Prokopenko, Dufosse, & Ouezdou, 2006; Itaguchi & Fukuzawa, 2012; Laboissiere, Lametti, & Ostry, 2009; Lametti, Houle, & Ostry, 2007; Wong, Wilson, Malfait, & Gribble, 2009a, 2009b). Although reflexes, voluntary muscle activity, muscle moment arms, and limb configuration all affect the orientation, shape, and area of stiffness ellipse and thus variability of hand position (Franklin et al., 2007; Krutky, Trumbower, & Perreault, 2013; Lametti et al., 2007; Prilutsky, 2000; Wong et al., 2009a), arm posture, musculoskeletal mechanics, and synergistic muscle control constrain possible changes in stiffness ellipse parameters, especially in the ellipse orientation (Hu, Murray, & Perreault, 2012; Inouye & Valero-Cuevas, 2016; Lametti & Ostry, 2010).

It appears from the above discussion that the precision of hand position sense and specifically the orientation of the precision ellipse should be closely related and orthogonal to the orientation of the stiffness ellipse at the same arm postures. The potential dependence of the precision of hand position sense on arm stiffness in position perception tasks and the extent to which such dependence is related to the transformation of joint to hand coordinates have not been fully appreciated and understood (Franklin et al., 2007; Itaguchi & Fukuzawa, 2012; Proske & Gandevia, 2018).

To examine how the measured arm stiffness ellipses would be related to the hand precision ellipses predicted by our geometric arm model, we plotted them together (Fig. 7) for the same 15 hand locations, for which stiffness was measured by Flash and Mussa-Ivaldi (1990). Since the subjects' arm segment lengths were not reported in that study, we used the following lengths of the forearm+hand and upper arm to compute the arm precision ellipses: L_{fa}= 32 cm and L_{ua} = 33 cm. These segment lengths were measured in one subject in the study (Mussa-Ivaldi et al., 1985), in which the same method of measuring arm stiffness was used. It can be seen that the arm precision and stiffness ellipses are nearly orthogonal to each other across the workspace. The mean difference in the direction of the major axis between the stiffness and precision ellipses was $78.0^{o} \pm 9.2^{o}$. The circular correlation coefficient (Jammalamadaka & SenGupta, 2001) between the two directions was 0.979. Interestingly, Lametti and Ostry (Lametti & Ostry, 2010) have reported the same average angle of 78^{o} between the major axes of the hand variability ellipse and the stiffness ellipse measured at the end of pointing movement to targets in a horizontal plane.

Thus, Fig. 7 supports findings of Itaguchi and Fukuzawa (Itaguchi & Fukuzawa, 2012) who measured distributions of variable errors of hand position sense and demonstrated that the long axis of those distributions were nearly orthogonal to the orientation of the major axis of stiffness ellipse measured at 4 hand locations of a single participant in study (Mussa-Ivaldi et al., 1985). They stressed importance of accounting for arm stiffness in evaluating results of proprioceptive assessments. Given the close association between the arm stiffness and hand precision ellipses, as demonstrated and discussed above, and the fact that arm stiffness parameters can be

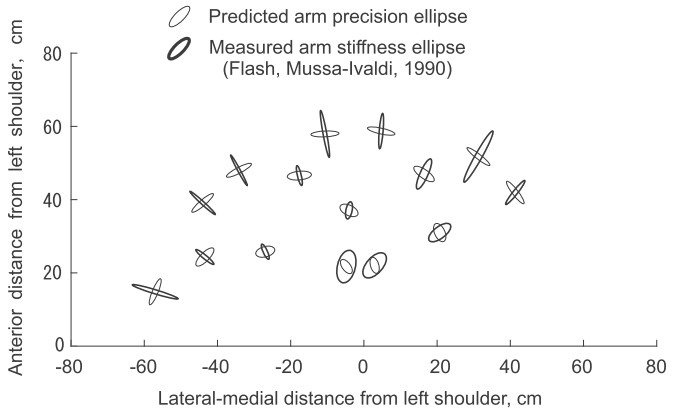

Fig. 7. Predicted hand precision ellipses and experimentally measured hand stiffness ellipses for the left arm. Stiffness ellipses were measured at 15 hand locations by Flash and Mussa-Ivaldi (1990) (see text for details).

voluntarily modulated by changing arm posture and muscle activity (Franklin et al., 2007; Frolov et al., 2006; Itaguchi & Fukuzawa, 2012; Lametti et al., 2007; Prilutsky, 2000; Trumbower, Krutky, Yang, & Perreault, 2009; Wong et al., 2009a, 2009b), we suggest that the hand precision ellipse parameters likewise can be actively modulated to improve precision of limb position sense to satisfy demands of various limb-position perceptual tasks. For example, the minor axis of the hand precision ellipse can be oriented in the direction that requires high precision of hand position sense by selecting an appropriate posture of the kinematically redundant arm, similar to orienting the arm stiffness ellipse in the desired direction to approve the performance of tracking tasks by selecting the appropriate arm postures (Trumbower et al., 2009). The size of the hand precision ellipse could be potentially decreased my muscle co-activation to improve overall precision of position sense, similar to improving precision of pointing tasks (Gribble et al., 2003). Thus, it appears possible to actively modulate precision of limb position sense through the process of active sensing that involves exploration and learning of the environment and constraints of the perceptual task, as well as motor planning and action (Yang, Wolpert, & Lengyel, 2018). This hypothesis of active sensing of limb position appears novel and is different from the concept of the 'fusimotor set' (Prochazka, Hulliger, Zangger, & Appenteng, 1985) because it allows for modulation of precision of hand position sense by adjusting kinematically redundant arm posture without changing stretch-sensitivity of the muscle spindles by the fusimotor action.

4.3. Limitations of the study

The results of our study are limited by the analysis of a simplified two degree-of-freedom (DOF) geometric model of the arm in a horizontal plane. The human arm has 7 major DOF (3 in shoulder, 2 in elbow, and 2 in wrist, if one does not count additional 7 DOF in the shoulder complex and over 15 DOF in the hand and digits), and all major DOF are involved in arm movement and postural tasks in three-dimensional space; e.g. (Zatsiorsky, 1998). We deliberately selected to investigate effects of the joint-to-hand coordinate transformation in a simple two-joint kinematic chain and used the corresponding experimental paradigm (see below) to make theoretical predictions more intuitive and easier to compare with experimental data. Thus, our results cannot be generalized to the three-dimensional space, and the contribution of the coordinate transformation to the non-uniform precision of position sense in frontal and sagittal planes remain uncertain. However, computer simulations of three-dimensional comprehensive neuromechanical models of the human arm (Hu et al., 2012; Inouye & Valero-Cuevas, 2016) have generally confirmed experimental findings (Krutky et al., 2013) that the orientation of hand stiffness ellipsoid, and thus the orientation of hand variability ellipsoid, is largely constrained in the three-dimensional space at a given arm posture.

In our experiments to test the precision of hand position sense, the participants matched the mirror position of the reference right hand by the matching left hand (Fig. 2A) instead of matching the same spatial location of the reference hand as typically done in hand position matching experiments (Itaguchi & Fukuzawa, 2012; Rincon-Gonzalez et al., 2011; Slinger & Horsley, 1906; van Beers et al., 1998). Matching the mirror position simplified the analysis and interpretation of the posture-dependent effects of coordinate transformation on the precision of hand position sense as arm postures (joint angles) of the two arms were essentially the same during matching. The hand position of each two-joint arm in a horizontal plane is defined by two independent coordinates in either external space (e.g., by hand Cartesian coordinates with respect to the initial hand position, see Fig. 2A) or in internal joint space (e.g., by shoulder and elbow angles). We explicitly instructed the participants "to match the distance and mirror direction of the right index finger motion from the initial position to the target with the left index fingertip". These instructions correspond to hand mirror-position matching in the external space. However, we cannot know whether the subjects strictly followed these instructions or they relied on matching the shoulder and elbow angles (posture matching) instead. Although the external and internal coordinates define the same hand position, the physiological mechanisms of matching the hand position in these two coordinate systems may be different. In the future, we intend to investigate potential differences in precision and accuracy of arm position sense between hand position matching in the external space and arm posture matching in internal joint coordinates.

5. Conclusion

The results of this study demonstrated that the nonlinear transformation of random errors in arm joint angles to random errors in hand coordinates contributed substantially to the non-uniform precision of hand position sense in the horizontal workspace. We investigated this transformation using a planar two-joint kinematic chain. This model predicted the orientation and elongated shape of hand precision ellipses that were consistent with those found experimentally in the hand mirror-position matching experiment. Although the model did not accurately predict the shape and area of the hand precision ellipse, it was still able to explain the non-uniform precision of hand position sense, i.e. higher precision in the radial (forward-backward) than azimuth (left-right) directions, as well as higher azimuth precision and lower radial precision for closer targets than for distant ones. Based on a close association between the orientation of hand precision and stiffness ellipses, we propose that precision of limb position sense can be improved by selecting an appropriate posture of the kinematically redundant arm and by setting specific muscle activity levels.

Data availability

The experimental datasets and computer code for data analysis are available from the corresponding author on reasonable request.

Funding

This research was supported by the US National Science Foundation grants EFRI-M3C 1137172 and ECCS- 2024414.

Author contributions

K.O.: Conceptualization, Data curation, Formal analysis, Investigation, Methodology, Software, Visualization, Validation, Writing - original draft, Writing - review and editing. B.I.P.: Conceptualization, Data curation, Formal analysis, Funding acquisition, Investigation, Methodology, Project administration, Resources, Supervision, Validation, Writing - original draft, Writing - review and editing.

Declaration of Competing Interest

The authors declare no competing interests.

Data availability

Data will be made available on request.

Acknowledgements

The authors thank Dr. Nikhilesh Natraj for help with data collection, Dr. Sanggyun Park for his advice on geometric analysis, and Dr. Teresa Snow for her advice on statistical analysis.

Appendix A. Supplementary data

Supplementary data to this article can be found online at https://doi.org/10.1016/j.humov.2022.103020.

References

Aimonetti, J. M., Hospod, V., Roll, J. P., & Ribot-Ciscar, E. (2007). Cutaneous afferents provide a neuronal population vector that encodes the orientation of human ankle movements. *The Journal of Physiology, 580*, 649–658.
Aimonetti, J. M., Roll, J. P., Hospod, V., & Ribot-Ciscar, E. (2012). Ankle joint movements are encoded by both cutaneous and muscle afferents in humans. *Experimental Brain Research, 221*, 167–176.
van Beers, R. J., Sittig, A. C., & Denier van der Gon, J. J. (1996). How humans combine simultaneous proprioceptive and visual position information. *Experimental Brain Research, 111*, 253–261.
van Beers, R. J., Sittig, A. C., & Denier van der Gon, J. J. (1998). The precision of proprioceptive position sense. *Experimental Brain Research, 122*, 367–377.
Bevan, L., Cordo, P., Carlton, L., & Carlton, M. (1994). Proprioceptive coordination of movement sequences: Discrimination of joint angle versus angular distance. *Journal of Neurophysiology, 71*, 1862–1872.
Bretscher, O. (2013). *Linear algebra with application* (5th ed.). Boston: Pearson.
Brown, L. E., Rosenbaum, D. A., & Sainburg, R. L. (2003). Limb position drift: Implications for control of posture and movement. *Journal of Neurophysiology, 90*, 3105–3118.
Clark, F. J., Larwood, K. J., Davis, M. E., & Deffenbacher, K. A. (1995). A metric for assessing acuity in positioning joints and limbs. *Experimental Brain Research, 107*, 73–79.
Cohen, L. A. (1958). Analysis of position sense in human shoulder. *Journal of Neurophysiology, 21*, 550–562.
Cole, J., & Paillar, J. (1998). Living without touch and peripheral information about body position and movement : Studies with deafferented subjects. In J. Bermúdez (Ed.), *The body and the self*. Cambridge, MA: MIT Press.
Collins, D. F., Refshauge, K. M., Todd, G., & Gandevia, S. C. (2005). Cutaneous receptors contribute to kinesthesia at the index finger, elbow, and knee. *Journal of Neurophysiology, 94*, 1699–1706.
Darling, W. G. (1991). Perception of forearm angles in 3-dimensional space. *Experimental Brain Research, 87*, 445–456.
Denavit, J., & Hartenberg, R. S. (1955). A kinematic notation for lower-pair mechanisms based on matrices. *American Society of Mechanical Engineers, 23*, 215–221.
Feldman, A. G. (2011). Space and time in the context of equilibrium-point theory. *Wiley Interdisciplinary Reviews: Cognitive Science, 2*, 287–304.
Flash, T., & Mussa-Ivaldi, F. (1990). Human arm stiffness characteristics during the maintenance of posture. *Experimental Brain Research, 82*, 315–326.
Franklin, D. W., Liaw, G., Milner, T. E., Osu, R., Burdet, E., & Kawato, M. (2007). Endpoint stiffness of the arm is directionally tuned to instability in the environment. *The Journal of Neuroscience, 27*, 7705–7716.
Frolov, A. A., Prokopenko, R. A., Dufosse, M., & Ouezdou, F. B. (2006). Adjustment of the human arm viscoelastic properties to the direction of reaching. *Biological Cybernetics, 94*, 97–109.
Fuentes, C. T., & Bastian, A. J. (2010). Where is your arm? Variations in proprioception across space and tasks. *Journal of Neurophysiology, 103*, 164–171.
Gribble, P. L., Mullin, L. I., Cothros, N., & Mattar, A. (2003). Role of cocontraction in arm movement accuracy. *Journal of Neurophysiology, 89*, 2396–2405.
Haggard, P., Newman, C., Blundell, J., & Andrew, H. (2000). The perceived position of the hand in space. *Perception & Psychophysics, 62*, 363–377.
Hakuta, N., Izumizaki, M., Kigawa, K., Murai, N., Atsumi, T., & Homma, I. (2014). Proprioceptive illusions created by vibration of one arm are altered by vibrating the other arm. *Experimental Brain Research, 232*, 2197–2206.
Hall, L. A., & McCloskey, D. I. (1983). Detections of movements imposed on finger, elbow and shoulder joints. *The Journal of Physiology, 335*, 519–533.
von Hofsten, C., & Rosblad, B. (1988). The integration of sensory information in the development of precise manual pointing. *Neuropsychologia, 26*, 805–821.
Hogan, N. (1985). The mechanics of multi-joint posture and movement control. *Biological Cybernetics, 52*, 315–331.
Howard, I. P. (1997). Interactions within and between the spatial senses. *Journal of Vestibular Research, 7*, 311–345.
Howard, I. S., Ingram, J. N., Kording, K. P., & Wolpert, D. M. (2009). Statistics of natural movements are reflected in motor errors. *Journal of Neurophysiology, 102*, 1902–1910.
Hu, X., Murray, W. M., & Perreault, E. J. (2012). Biomechanical constraints on the feedforward regulation of endpoint stiffness. *Journal of Neurophysiology, 108*, 2083–2091.
Inglis, J. T., Frank, J. S., & Inglis, B. (1991). The effect of muscle vibration on human position sense during movements controlled by lengthening muscle contraction. *Experimental Brain Research, 84*, 631–634.
Inouye, J. M., & Valero-Cuevas, F. J. (2016). Muscle synergies heavily influence the neural control of arm endpoint stiffness and energy consumption. *PLoS Computational Biology, 12*, Article e1004737.

Itaguchi, Y., & Fukuzawa, K. (2012). Effects of arm stiffness and muscle effort on position reproduction error in the horizontal plane. *Perceptual and Motor Skills, 114*, 757–773.
Jammalamadaka, S. R., & SenGupta, A. (2001). *Topics in circular statistics*. River Edge, N.J.: World Scientific.
Johnson, R. A., & Wichern, D. W. (2007). *Applied multivariate statistical analysis* (6th ed.). Upper Saddle River, NJ: Pearson Education Inc.
Krutky, M. A., Trumbower, R. D., & Perreault, E. J. (2013). Influence of environmental stability on the regulation of end-point impedance during the maintenance of arm posture. *Journal of Neurophysiology, 109*, 1045–1054.
Kuling, I. A., van der Graaff, M. C., Brenner, E., & Smeets, J. B. (2017). Matching locations is not just matching sensory representations. *Experimental Brain Research, 235*, 533–545.
Laboissiere, R., Lametti, D. R., & Ostry, D. J. (2009). Impedance control and its relation to precision in orofacial movement. *Journal of Neurophysiology, 102*, 523–531.
Lackner, J. R. (1984). Some influences of tonic vibration reflexes on the position sense of the contralateral limb. *Experimental Neurology, 85*, 107–113.
Lametti, D. R., Houle, G., & Ostry, D. J. (2007). Control of movement variability and the regulation of limb impedance. *Journal of Neurophysiology, 98*, 3516–3524.
Lametti, D. R., & Ostry, D. J. (2010). Postural constraints on movement variability. *Journal of Neurophysiology, 104*, 1061–1067.
Lonn, J., Crenshaw, A. G., Djupsjobacka, M., & Johansson, H. (2000). Reliability of position sense testing assessed with a fully automated system. *Clinical Physiology, 20*, 30–37.
Matthews, P. B. (1988). Proprioceptors and their contribution to somatosensory mapping: Complex messages require complex processing. *Canadian Journal of Physiology and Pharmacology, 66*, 430–438.
Maybeck, P. S. (1979). *Stochastic models, estimation, and control. 1*. New York: Academic Press.
Merlet, J.-P. (2006). Jacobian, manipulability, condition number, and accuracy of parallel robots. *Journal of Mechanical Design, 128*, 199.
Mussa-Ivaldi, F. A., Hogan, N., & Bizzi, E. (1985). Neural, mechanical, and geometric factors subserving arm posture in humans. *The Journal of Neuroscience, 5*, 2732–2743.
Oldfield, R. C. (1971). The assessment and analysis of handedness: The Edinburgh inventory. *Neuropsychologia, 9*, 97–113.
Plooy, A., Tresilian, J. R., Mon-Williams, M., & Wann, J. P. (1998). The contribution of vision and proprioception to judgements of finger proximity. *Experimental Brain Research, 118*, 415–420.
Prilutsky, B. I. (2000). Coordination of two- and one-joint muscles: Functional consequences and implications for motor control. *Motor Control, 4*, 1–44.
Prochazka, A., Hulliger, M., Zangger, P., & Appenteng, K. (1985). "Fusimotor set": New evidence for alpha-independent control of gamma-motoneurones during movement in the awake cat. *Brain Research, 339*, 136–140.
Proske, U. (2015). The role of muscle proprioceptors in human limb position sense: A hypothesis. *Journal of Anatomy, 227*, 178–183.
Proske, U., & Gandevia, S. C. (2012). The proprioceptive senses: Their roles in signaling body shape, body position and movement, and muscle force. *Physiological Reviews, 92*, 1651–1697.
Proske, U., & Gandevia, S. C. (2018). Kinesthetic senses. *Comprehensive Physiology, 8*, 1157–1183.
Ribot-Ciscar, E., Bergenheim, M., Albert, F., & Roll, J. P. (2003). Proprioceptive population coding of limb position in humans. *Experimental Brain Research, 149*, 512–519.
Rincon-Gonzalez, L., Buneo, C. A., & Helms Tillery, S. I. (2011). The proprioceptive map of the arm is systematic and stable, but idiosyncratic. *PLoS One, 6*, Article e25214.
Rossetti, Y., Meckler, C., & Prablanc, C. (1994). Is there an optimal arm posture? Deterioration of finger localization precision and comfort sensation in extreme arm-joint postures. *Experimental Brain Research, 99*, 131–136.
Sainburg, R. L., Poizner, H., & Ghez, C. (1993). Loss of proprioception produces deficits in interjoint coordination. *Journal of Neurophysiology, 70*, 2136–2147.
Sarlegna, F. R., Gauthier, G. M., Bourdin, C., Vercher, J. L., & Blouin, J. (2006). Internally driven control of reaching movements: A study on a proprioceptively deafferented subject. *Brain Research Bulletin, 69*, 404–415.
Scott, S. H., & Loeb, G. E. (1994). The computation of position sense from spindles in mono- and multiarticular muscles. *The Journal of Neuroscience, 14*, 7529–7540.
Simani, M. C., McGuire, L. M., & Sabes, P. N. (2007). Visual-shift adaptation is composed of separable sensory and task-dependent effects. *Journal of Neurophysiology, 98*, 2827–2841.
Slinger, R. T., & Horsley, V. (1906). Upon the orientation of points in space by the muscular, arthrodial, and tactile senses of the upper limbs in normal individuals and in blind persons. *Brain, 29*, 1–27.
Soechting, J. F. (1982). Does position sense at the elbow reflect a sense of elbow joint angle or one of limb orientation? *Brain Research, 248*, 392–395.
Soechting, J. F., & Ross, B. (1984). Psychophysical determination of coordinate representation of human arm orientation. *Neuroscience, 13*, 595–604.
Spong, M. W., & Vidyasagar, M. (1989). *Robot dynamics and control*. New York: Wiley.
Sturnieks, D. L., Wright, J. R., & Fitzpatrick, R. C. (2007). Detection of simultaneous movement at two human arm joints. *The Journal of Physiology, 585*, 833–842.
Trumbower, R. D., Krutky, M. A., Yang, B. S., & Perreault, E. J. (2009). Use of self-selected postures to regulate multi-joint stiffness during unconstrained tasks. *PLoS One, 4*, Article e5411.
Wilson, E. T., Wong, J., & Gribble, P. L. (2010). Mapping proprioception across a 2D horizontal workspace. *PLoS One, 5*, Article e11851.
Wong, J., Wilson, E. T., Malfait, N., & Gribble, P. L. (2009a). The influence of visual perturbations on the neural control of limb stiffness. *Journal of Neurophysiology, 101*, 246–257.
Wong, J., Wilson, E. T., Malfait, N., & Gribble, P. L. (2009b). Limb stiffness is modulated with spatial accuracy requirements during movement in the absence of destabilizing forces. *Journal of Neurophysiology, 101*, 1542–1549.
Yang, S. C., Wolpert, D. M., & Lengyel, M. (2018). Theoretical perspectives on active sensing. *Current Opinion in Behavioral Sciences, 11*, 100–108.
Zatsiorsky, V. M. (1998). *Kinematics of human motion*. Champaign, IL: Human Kinetics.